Modulation of Cytochrome C Coupling to Anionic Lipid Monolayers by a Change of the Phase State: A Combined Neutron and Infrared Reflection Study

Andreas P. Maierhofer,* David G. Bucknall,† and Thomas M. Bayerl*
*Universität Würzburg, Physikalisches Institut EP5, 97074 Würzburg, Germany and †Rutherford Appleton Laboratory, ISIS Chilton, United Kingdom

ABSTRACT The effect of monolayer domain formation on the electrostatic coupling of cytochrome c from the subphase to a monolayer at the air/water interface was studied using a combination of neutron reflection (NR) and infrared reflection absorption spectroscopy (IRRAS) techniques. The monolayers consisted of a binary mixture of the zwitterionic phosphatidylcholine and the anionic phosphatidylglycerol. For a monolayer of dipalmitoylphosphatidylcholine (DPPC) and dimyristoylphosphatidylglycerol (DMPG, 30 mol%), which exhibits a non-ideal mixing of the two lipid components, we observed a significantly higher protein coupling to the liquid-condensed phase compared to the liquid-expanded state. In contrast, this higher protein binding was not observed when the two lipids had identical chain lengths (nearly ideal mixing). Similarly, for an equimolar mixture of DPPC and DMPG, we did not observe significant differences in the protein binding for the two phase states. The results strongly suggest that the domain formation in a condensed monolayer under non-ideal lipid mixing conditions is crucial for the cytochrome c binding strength. Furthermore, this study demonstrates the significant advantages of gathering information on protein–monolayer coupling by the combined use of a dedicated IRRAS set-up with the NR technique.

INTRODUCTION

The phase transition of phospholipid monolayers at the air/water interface between a fluid-like liquid expanded (LE) and a more solid-like liquid condensed (LC) phase is a well-known phenomenon and has been studied in great detail over the past two decades (Albrecht et al., 1978; Möhwald, 1995). The transition from the LE to the LC phase is connected with the formation of micron size, crystal-like domains at lateral pressures above the transition point, which can be readily observed by fluorescence or Brewster angle microscopic methods (Möhwald, 1995). For monolayers consisting of more than one lipid species, the domain formation may lead to a partial demixing of the lipids, i.e., an enrichment of one species within the domain at the expense of the other species. If one of these species carries an excess electric charge while the other is zwitterionic or neutral, the demixing is equivalent to the creation of a heterogeneous distribution of surface charge density over the monolayer. In contrast, under LE phase conditions, this charge distribution can be expected to be homogenous owing to the lateral diffusion of the lipids (Peters and Beck, 1983).

This change of surface charge distribution between LE and LC phase may lead to differences in the partition of water-soluble proteins undergoing a Coulomb attraction by the monolayer between the surface and the subphase. Thus, it seems feasible that, under certain conditions, electrostatic protein binding and unbinding to or from the monolayer can be controlled by its phase state. For phospholipid bilayers on a solid support, we demonstrated recently that this concept of the modulation of protein binding by the lipid phase state is indeed functional (Käsbauer and Bayerl, 1999) and can be used for the advanced separation (phase transition chromatography) of proteins (Loidl-Stahlhofen et al., 1996).

The aim of this work is to provide evidence that a similar mechanism exists in lipid monolayers at the air/water interface and with proteins dissolved in the subphase. To detect differences in the amount of proteins attached to the monolayer as a function of its phase state, we used two surface-sensitive methods that are both well established for the study of monolayer systems: neutron reflection (NR) and infrared reflection-absorption spectroscopy (IRRAS). The introduction of a trough shuttle technique for IRRAS, as previously suggested by Flach et al. (1994), allowed, in our setup, for an optimum compensation of rotational water-absorbance bands. This enabled reproducible measurements of protein adsorption to monolayers over a long time range (up to 10 h). The combined application of these methods allows detailed information about the structure and density of the bound protein layer to be obtained and thus gives information on the amount of protein bound to the monolayer. The water-soluble protein selected for this study was cytochrome c because it has been used in the previous bilayer studies (Käsbauer and Bayerl, 1999) and a detailed knowledge is available on its structure and electrostatic nature of its interaction with lipid surfaces.

Received for publication 29 November 1999 and in final form 30 May 2000.

Address reprint requests to Prof. Thomas M. Bayerl, Universität Würzburg, Physikalisches Institut EP-5, D-97074 Würzburg, Germany. Tel.: +49-931-8885863; Fax: +49-931-8885851; E-mail: bayerl@physik.uni-wuerzburg.de.

0006-3495/00/09/1428/10 $2.00

MATERIALS AND METHODS

Materials

All lipids were purchased from Avanti Polor Lipids (Alabaster, AL) and were dissolved in a 9:1 chloroform/methanol solution at a concentration of 1 nmol/μl. From these solutions, the binary mixtures listed in Table 1 were prepared volumetrically.

All experiments involving cytochrome c were carried out using a subphase of D_2O (for NR, 99.9% purity from Fluorchem Ltd., Old Glossop, UK; for IRRAS, 97.5% purity from Deuchem GmbH, Leipzig, Germany), which was buffered at pH 7.0 $\pm$ 0.1 with 20 mM HEPES and 0.25 mM EDTA. Experiments on pure lipid monolayers were performed using D_2O and H_2O (Millipore purified water) buffered subphases as described above.

Cytochrome c was obtained from Fluka (Deisenhofen, Germany) and was dissolved in an aliquot of the buffer at concentrations of up to 2 mg/ml. The dissolution was done at least 2 h in advance of the NR or IRRAS experiments to allow labile protons to exchange with deuterons from the buffer.

Lipid monolayers were spread from the organic solution using a microsyringe and, afterwards, compressed to the desired surface pressure. For both the NR and the IRRAS experiments, Langmuir troughs were used, which allow the pressure-tight sealing of an inner "protein compartment" after compression by closing a 2-mm wide channel link with a teflon plate (Naumann et al., 1996). This procedure avoids film leakage and allows a better control of the protein concentration in the subphase.

The maximum subphase surface area of the Langmuir troughs was 289 cm^2 and 223 cm^2 for the NR and IRRAS experiments, respectively. The inner protein compartments had areas and volumes of 64.5 cm^2 and 38.5 $\pm$ 2.5 ml for NR and of 49.7 cm^2 and 27.5 $\pm$ 2.5 ml for IRRAS. The subphase was kept at 20.0 $\pm$ 0.2°C for all experiments.

Methods

NR was measured at the CRISP spectrometer of the ISIS spallation source (Rutherford-Appleton Laboratory, Chilton, U.K.) according to procedures previously described in detail (Maierhofer and Bayerl, 1998; Naumann et al., 1994). For each experiment, lipid monolayers were prepared in the LE or LC phase, and the channel link was closed after compression. Reflectivity curves were recorded first for the pure lipid monolayer without protein in the subphase. After this, up to 300 μl cytochrome c solution was injected into the subphase through submersed injection holes located in the edge of the inner protein compartment. After 40 min. incubation time, NR measurements were performed. The final cytochrome c concentration was $c_0 = 420 \pm 30$ nM in all experiments but for 50:50 DPPC-d62:DMPG-d54 in LC phase. Throughout the whole experiment, the lateral pressure π was recorded to ensure that equilibrium conditions were reached before the commencement of NR measurements. To aid data analysis of NR measurements on a D_2O subphase, samples of the subphase were collected during the experiments and their isotopic purity checked by proton nuclear magnetic resonance, which accurately quantified any changes in subphase neutron scattering length due to unavoidable atmospheric H–D exchange.

TABLE 1 Composition of all lipid monolayer samples studied

% PG	Sample Composition	Method
30	70:30 mol% DPPC-d62:DMPG	NR, IRRAS
	70:30 mol% DPPC-d62:DMPG-d54	NR
	70:30 mol% DMPC:DMPG	IRRAS
	70:30 mol% DPPC-d62:DPPG	IRRAS
50	50:50 mol% DPPC-d62:DMPG	NR, IRRAS
	50:50 mol% DPPC-d62:DMPG-d54	NR
80	20:80 mol% DPPC:DPPG-d62	NR, IRRAS

To achieve the highest possible precision in the quantification of the amount of adsorbed protein, mixtures of lipids with their alky chain perdeuterated analogs were used. This allowed the optimization of the scattering length density (SLD) contrast between the lipid monolayer and the adsorbed cytochrome c monolayer. For an improved characterization of the lipid monolayer itself, additional NR data were gathered on monolayers of identical chemical composition but at different proportions of chain perdeuterated lipid analogs in the monolayer and on different subphases (D_2O and H_2O), thus enabling a thorough contrast variation.

IRRAS measurements were performed using a Perkin-Elmer Spectrum 2000 spectrometer with a liquid N_2-cooled MCT detector. For each spectrum, 512 interferograms were acquired at a resolution of 4 cm^{-1} (acquisition time ~9 min). The system was equipped with a user-modified Specac (LOT, Langenberg, Germany) external reflection unit and a home-built film balance. The angle of incidence was 28° with respect to the surface norm. To maintain a constant water-vapor content and temperature, the set-up was placed in a hermetically sealed and thermal insulated sample container. The change of water level in the trough due to evaporation during the experiment was found to be negligible. Spreading of the lipid monolayers and injection of the protein solution were achieved by operating through small holes without opening the sample container.

Measurements were done by switching between two troughs at regular intervals (every 10 min) at the beam position using a home-built trough shuttle system controlled by the acquisition computer. One trough equipped with the inner protein compartment contained the monolayer system under study (sample), whereas the other (reference) was filled with the pure subphase. The shuttle motion did not cause any additional changes of the lateral pressure in the sample trough during the experiment compared to a trough kept fixed for the same time. Reflection-absorbance (RA) spectra were generated from subsequent sample and reference measurements using GRAMS Version 3.01 software (Galactic Industries Corp., Salem, NH). Here, RA is defined as $RA = -\log(R_S/R_R)$, where R_S and R_R represent the reflectance of the sample and of the reference compartment, respectively. Each experiment consisted of a first step of typically 5 RA spectra recorded for the pure lipid monolayer without protein in the subphase ("lipid spectra"). Afterwards, up to 154 μl cytochrome c solution were injected to the subphase and allowed to equilibrate. The final concentration in all experiments was $c_0 = 420 \pm 30$ nM. Then, in a second step, the "protein spectra" were recorded over a total time of up to 10 h.

Because H_2O exhibits a strong absorbance in the amide I region (1700–1600 cm^{-1}), it is unsuitable for quantitative comparisons. Therefore, all IRRAS experiments were conducted with D_2O as a subphase, which shows only weak absorption in the amide I region.

After the injection of protein solution into the subphase, spectral features of the amide I bands became visible in the RA spectra. To remove the contributions of the lipid monolayer and the bulk water in the amide I region and to improve the compensation of water vapor bands, difference spectra were calculated from the protein spectra and the lipid spectra (see Data Analysis section).

DATA ANALYSIS

NR data

NR data were analyzed by least square fitting of multilayer models to the reflectivity curves using the program MULF, which implements the optical matrix method (Born and Wolf, 1993). Each layer in the fit is characterized by its thickness d_j, its SLD ρ_j, and a Gaussian roughness σ_j. In our case, all fits were performed with $\sigma_j = 0$.

To characterize the pure lipid monolayer in terms of a head-group and a chain region, a two-layer model (four-parameter fit) was used as previously described in detail

(Naumann et al., 1994, 1995). To reduce ambiguity due to the four free parameters, additional constraints were used:

1. The head group thickness was kept constant for all experiments at $d_{Hd} = 8.0$ Å. This value was consistent with a reasonable structural interpretation of the data (see below) and is in agreement with previous data of binary lipid monolayers (Bayerl et al., 1990) and DPPC bilayers (Nagle and Wiener, 1988).

2. The area per lipid molecule $A_{Lip,\ calc}$ calculated from the NR data fitting according to

$$A_{Lip,calc} = b_{Ch}/\rho_{Ch}d_{Ch} \quad (1)$$

(b_{Ch}, calculated scattering length of chain region; ρ_{Ch}, fitted SLD of chain region; d_{Ch}, fitted thickness of the chain region) was required to agree with the area per lipid molecule $A_{Lip,ex}$ obtained from the film balance measurements within a confidence limit of 8%. This rather wide error limit also accounts for possible uncertainties in b_{Ch} by mixing deuterated and protonated lipids. Errors of the model fits were determined from an analysis of the variation of the fit quality parameter χ^2 (Naumann et al., 1994, 1995) for different model fits to the data. Error limits of the fit parameters were taken from those fits that caused an increase of χ^2 by 10% from its minimum value.

The presence of the protein for the case of the monolayer with cytochrome c in the subphase was considered as a third layer (Naumann et al., 1996; Johnson et al., 1991) with the parameters d_{Pr} (thickness of protein layer) and ρ_{Ch} (SLD of protein layer). In the fitting process of this three-layer system, the values obtained for the pure lipid layer were taken as initial values for the fits. Because no expansion of the lipid film could occur upon protein absorption due to the closure of the protein compartment, the same boundary conditions as for the pure lipid monolayer, i.e., d_{Hd} fixed and $A_{Lip,calc}$ in agreement with $A_{Lip,ex}$, were applied, and error limits of the fit parameters were obtained as above.

Summing up, data were fit with three free parameters and one boundary condition for the pure lipid monolayer and with five free parameters and one boundary condition for the lipid monolayer plus adsorbed protein. As in the latter case, the total layer thickness increased to more than 5 nm, this procedure always led to unique solutions for the free parameters (Johnson et al., 1991; Brumm et al., 1994; Naumann et al., 1994).

From the fitting results the value η_{Pr}, the fraction of protein in the protein layer,

$$\eta_{Pr} = (\rho_W - \rho_{Pr})/(\rho_W - \rho_{Pr,0}) \quad (2)$$

was calculated. Here, ρ_W is the SLD of the subphase and $\rho_{Pr,0}$ is the SLD of the pure protein, considering that $\rho_{Pr,0}$ is a function of ρ_W owing to the exchange of labile protons in the protein.

A gradual decrease of the isotopic enrichment of the D_2O subphase by vapor exchange, as determined by high-resolution proton NMR, was considered in the data analysis. In the course of a typical NR experiment, ρ_W decreased from its initial value of $\rho^{(99.8\%\ D2O)} = 6.36 \cdot 10^{-6}$ Å^{-2} by up to $0.4 \cdot 10^{-6}$ Å^{-2}. The correction introduced for ρ_W altered the values for η_{Pr} by less than 6%.

IRRAS data

Although the lipid monolayer exhibits no absorbance in the amide I region of the IRRAS, it can be shown by simulations of the IRRAS spectra using the optical multilayer model (Dluhy, 1986) that monolayers with different values of the real part n of their complex refractive index $n = n_j + i\kappa_j$ lead to distinct features in the spectra under conditions that the subphase imaginary part κ is nonvanishing. If these features arise in the amide I peak region of an adsorbed protein layer, its peak height will not solely depend on the amount of protein adsorbed but also on the refractive index n of the lipid monolayer. Because n depends on the monolayer density, which in turn is closely related to the area per lipid molecule, identical amounts of adsorbed protein would give rise to different amide I peak heights in the LE and the LC phase.

This behavior of the amide I band was corrected for by subtracting the spectrum of the pure lipid monolayer from that of the same monolayer (and at the same lateral pressure) with protein adsorbed. This kind of first-order correction worked satisfactorily for D_2O subphases only where κ is sufficiently small (Bertie et al., 1989).

For each set of protein data, those difference spectra that showed the least disturbance by water vapor bands were selected for further analysis, resulting in the selection of typically 20 difference spectra calculated from 10 protein spectra. For each selected difference spectrum in the region between 2000 and 1500 cm^{-1}, the peak height of the amide I band was obtained from fitting two Gaussians (corresponding to the absorption bands of amide I at $\approx$1650 cm^{-1} and a band attributed to vibrations of aspartic acid and arginine side chains (Flach et al., 1994; Chirgadze et al., 1975)) and a linear baseline. Peak heights were averaged over up to 18 difference spectra calculated with the same lipid spectrum.

RESULTS

We studied monolayers of PC-PG mixtures that contained 30, 50, or 80% of the anionic lipid to evaluate the dependence of cytochrome c binding on the monolayer charge. To consider additionally the effect of lipid demixing on protein binding, we studied monolayers where the chain lengths of the two lipids mismatched (C14 chains for PG, C16 chains for PC) and compared them with systems without mismatch (C16 or C14 chains for both PC and PG). Further differences between the samples studied were due to isotopic

substitutions of the lipid chains by their perdeuterated analogs. This enabled scattering contrast optimization with the aim of a high fidelity of the adsorbed protein quantification by NR. The exact compositions of all samples used in this work are listed in Table 1.

Anionic monolayers without proteins

The compression isotherms of all binary mixtures used are shown in Fig. 1 with the positions marked at which NR and IRRAS measurements were performed before and after protein addition to the subphase. The isotopic substitution of the lipids according to Table 1 caused only slight deviations from the isotherms shown. For example, the replacement of DMPG by DMPG-d54 caused a shift of the transition point toward higher pressure of <1 mN/m while retaining the shape of the isotherm (data not shown). Representative examples of NR curves without and with adsorbed protein are shown in Fig. 2.

For the monolayers containing 30 and 50 mol% DMPG, both NR and IRRAS showed the expected changes upon the transition from the LE to the LC phase state: From the NR point of view, the transition caused an increase of the chain region thickness of $\Delta d_{Ch} \approx 4$ Å in both D_2O and H_2O contrast (cf. Table 2). The absolute values of monolayer thickness and SLD as summarized in Table 2 compare well with those of previous publications (Maierhofer and Bayerl, 1998; Brumm et al., 1994; Naumann et al., 1994).

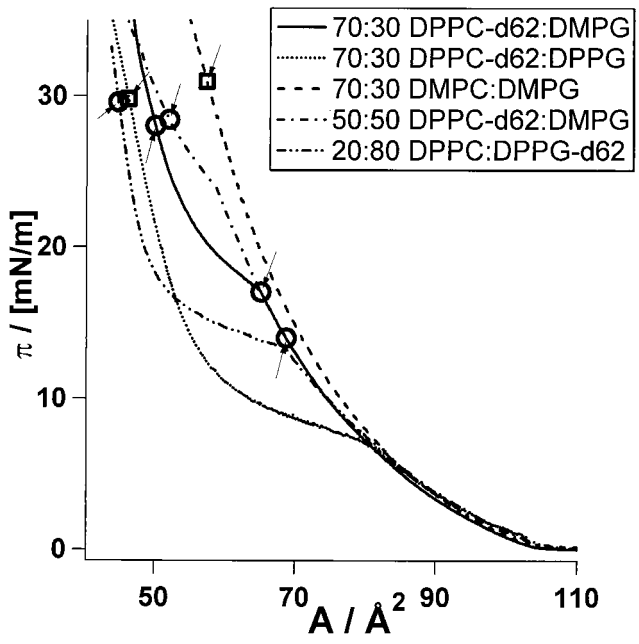

FIGURE 1 Pressure-area isotherms (compression mode) of the binary PC/PG monolayers studied. The arrows indicate the positions at which NR and IRRAS measurements (*circles*) or IRRAS measurements only (*squares*) were performed before and after protein addition.

The IRRAS technique allowed a simultaneous observation of the DPPC-d62 and the DMPG component upon the LE-LC transition. This phase transition caused a shift $\Delta\bar{\nu}$ to lower wave numbers for the asymmetric C-D ($\bar{\nu}_{LE} = 2127.5 \pm 0.5$ cm^{-1}, $\Delta\bar{\nu} = -2.35 \pm 0.45$ cm^{-1}) and C-H ($\bar{\nu}_{LE} = 2926.0 \pm 0.5$ cm^{-1}, $\Delta\bar{\nu} = -3.5 \pm 0.6$ cm^{-1}) stretching mode. The observed shift took place over a pressure range that coincided with the coexistence region of the monolayer as represented in Fig. 1. Furthermore, the total shift in wavenumber compares well to that observed for phospholipid bilayers of similar composition at the fluid/gel transition (Reinl and Bayerl, 1993).

Protein adsorption from the subphase

Adsorption kinetics and layer structure

Addition of cytochrome c to the subphase resulted in an increase in surface pressure $\Delta\pi$ of up to 8 mN/m for LE phase conditions and up to 6 mN/m for the LC phase conditions (cf. Table 3). For monolayer experiments within the same phase state (either LE or LC), this increase of $\Delta\pi$ scaled with the amount of anionic PG present in the monolayer and required up to 2 h for full equilibration, whereas 95% of the $\Delta\pi$ change occurred within 40 min.

Measuring the absorption kinetics using IRRAS by recording the amide band intensity versus time, we observed that, 40 min after protein addition, the amide I band intensity had reached equilibrium. Over the same time range we observed significant changes in the neutron specular reflection of the monolayer, whereas longer equilibration time did not result in further alterations of the reflectivity curve. From the NR (Fig. 2), we obtained a mean thickness $\langle d_{Pr} \rangle$ of the cytochrome c layer in all experiments of 27 ± 2 Å (see Table 4). Neither the increase of the anionic lipid content from 30 to 80% nor a chain mismatch between the two lipid components (PC and PG) caused changes of $\langle d_{Pr} \rangle$ beyond the error limit of ± 2 Å. Even protein concentrations in the subphase of up to 700 nM, corresponding to an approximate 20-fold excess of the amount of cytochrome c required for a closely packed single protein layer beneath the lipid monolayer, did not affect this result. This clearly indicates that a single protein layer is formed under all conditions and that excess protein does not lead to a stacking of protein layers.

Our value of $\langle d_{Pr} \rangle$ is about 10% smaller than the mean diameter of cytochrome c of 31 Å, as determined by x-ray crystallography (Bushnell and Louie, 1990). This may either be caused by a rather weak neutron scattering contrast of some amino acid side chains exposed to the cytochrome c surface or by a partial penetration of the protein of less than 4 Å into the head group region of the monolayer.

Determination of the amount of bound cytochrome c

From the NR, the amount of bound cytochrome c was determined directly from the data-fitting procedure accord-

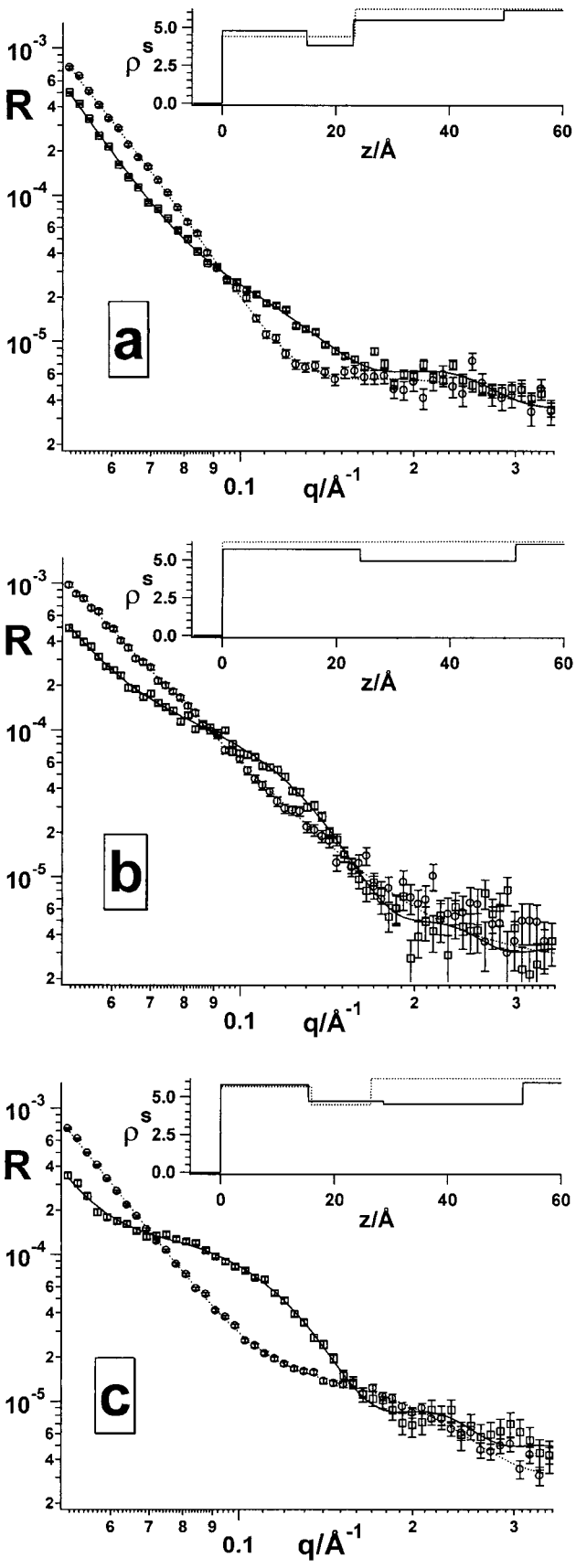

ing to Eq. 2 as the fraction η_{Pr} of protein in the protein layer. In contrast, IRRAS is restricted to a relative comparison of bound protein. This is mainly because changes of conformation and orientation of the protein may influence the IR absorbance, rendering the assignment of a "specific absorbance" to a given protein faulty. Furthermore, no information on the protein layer thickness is provided by IRRAS. Hence, multilayer adsorption becomes indistinguishable from closer molecular packing within a monolayer. However, in combination with NR, these shortcomings of IRRAS can be bypassed.

Figure 3 shows the amide I absorbance of cytochrome c adsorbed to the different lipid monolayer samples. For a comparison with the NR data, the IRRAS amide I peak heights were calibrated using the η_{Pr} value obtained from NR for the monolayer containing 80% PG, the system with the highest binding of cytochrome c. Here we assumed that the same amount of cytochrome c was adsorbed in both IRRAS and NR experiments at 80% PG. The results obtained by this approach are summarized in Table 5. The equivalence of the two methods for the determination of the amount of protein bound becomes obvious by plotting η_{Pr} obtained by IRRAS and NR as a function of the anionic lipid content (Fig. 4): The values agreed very well within the error limits of the two methods.

To exclude that any orientational change of cytochrome c is connected with the increase of monolayer charge density that might influence the height of the amide I absorbance, polarized IR measurements were performed as a function of monolayer PG content. From that, the dichroic ratio $D = RA_p/RA_s$ of the amide I band was calculated (RA_p, RA_s: absorbance of p- and s- polarized IR radiation, respectively) for the different PG contents. For all samples containing either 30 or 50% PG, we obtained $D = 1.19 \pm 0.04$. Thus, no significant change of cytochrome c orientation with a denser packing in the adsorbed protein monolayer was indicated by the IR dichroic ratio. A similar conclusion regarding the largely unchanged orientation of cytochrome c was reached previously by other authors by Raman scattering (Macdonald and Smith, 1996). Our approach to combine IRRAS and NR for protein layer quantification has the distinct advantage that, after the calibration of selected IRRAS data by the beam-time restricted NR method has been achieved, the IRRAS can be used for the systematic study of the system on the lab bench.

FIGURE 2 Neutron reflection curves of selected binary PC/PG monolayers before (*circles*) and after (*squares*) cytochrome c adsorption. The lines represent the best fits of 2-layer models (pure lipid monolayers, *dotted lines*) and of 3-layer models (after cytochrome c adsorption, *solid lines*). The inserts show the SLD profiles obtained from these models. *A.* 70:30 DPPC-d62:DMPG, LE phase. *B.* 50:50 DPPC-d62:DMPG-d54, LC phase. *C*, 20:80 DPPC:DPPG-d62, LC phase.

TABLE 2 Characterization of the pure lipid monolayers in terms of their chain and headgroup region thickness (d_{Ch} and d_{Hd}) and SLD (ρ_{Ch} and ρ_{Hd}) as derived from two-layer model fits of the NR data

Sample	Lipid Phase	A_{mol}/Å^2	Subphase	d_{Ch}/Å	$\rho_{Ch}/10^{-6}$ Å^{-2}	d_{Hd}/Å	$\rho_{Hd}/10^{-6}$ Å^{-2}
70:30 DPPC-d62:DMPG	LE	64 ± 3	D_2O	14.8 ± 1.8	4.50 ± 0.18	8.0	4.30 ± 0.48
70:30 DPPC-d62:DMPG-d54	LC	48 ± 2	D_2O	18.3 ± 1.8	6.66 ± 0.07	8.0	6.06 ± 0.01
			H_2O	19.0 ± 1.5	6.07 ± 0.06	8.0	2.99 ± 0.99
50:50 DPPC-d62:DMPG	LE	66 ± 2	D_2O	10.9 ± 1.9	4.42 ± 0.49	8.0	3.86 ± 0.54
50:50 DPPC-d62:DMPG-d54		69 ± 2	H_2O	13.5 ± 1.5	6.13 ± 0.19	8.0	2.35 ± 0.83
50:50 DPPC-d62:DMPG	LC	52 ± 1	D_2O	14.5 ± 2.0	4.68 ± 0.44	8.0	3.46 ± 0.62
50:50 DPPC-d62:DMPG-d54			H_2O	19.0 ± 2.0	5.98 ± 0.12	8.0	2.26 ± 1.19
20:80 DPPC:DPPG-d62	LC	45 ± 2	D_2O	18.5 ± 1.0	5.58 ± 0.10	8.0	4.29 ± 0.18

Confidence limits for the fitting results were determined as described in the Data Analysis section.
A_{mol}: area per lipid molecule obtained from three independent film balance measurements.

Effect of monolayer phase state and lipid chain mismatch

The above approach for the quantification of bound protein was further used to study the influence of the phase state on the cytochrome c binding. For a mixture containing 30 mol% anionic DMPG, we observed a significant difference in protein binding between the LC and the LE phase. As can be seen from Table 4, the protein coverage η_{Pr} measured by NR was 20% in the LE and 32% in the LC phase. This increase in protein binding under LC phase conditions was confirmed by IRRAS (Table 5), where an increase of η_{Pr} from 21 to 30% was observed, thus similar to the increase measured by NR.

In contrast, for 50% anionic DMPG in the monolayer, only a slight tendency toward enhanced protein binding in the LC phase was observed by IRRAS. From the NR point of view, an increase of η_{Pr} from 36.5 to 41.8% (Table 4) was observed between LE and LC phase. However, this apparent increase must be accounted at least in part to the higher protein subphase concentration at which the LC phase NR measurement was performed (700 nM (LC) rather than 420 nM (LE) cytochrome c). Systematic NR studies of the effect of protein subphase concentration c_S on η_{Pr} under LC phase conditions showed, for 50% DMPG monolayers, an increase of η_{Pr} with c_S: We obtained η_{Pr} = 35.5, 37.5, and 41.8% for protein subphase concentrations c_S = 210, 294, and 700 nM, respectively. Interpolation of the η_{Pr} values for c_S = 420 nM (the c_S at which the LE phase measurement was done) gave a coverage of 39.5% for the LC phase, thus a slight increase by 3% in agreement with the IRRAS result (Table 5).

TABLE 3 Initial monolayer lateral pressure π_0 and the pressure increase $\Delta\pi$ after the injection of cytochrome c to the subphase at a concentration of 420 ± 30 nM for all monolayer samples studied

Sample	Lipid Phase	π_0	$\Delta\pi$
70:30 DPPC-d62:DMPG	LE	15.8 ± 1.8	3.1 ± 1.6
	LC	30.2 ± 1.1	2.6 ± 0.5
70:30 DMPC:DMPG	LE	30.9 ± 0.6	5.0 ± 0.5
70:30 DPPC-d62:DPPG	LC	29.8 ± 0.8	4.4 ± 0.5
50:50 DPPC-d62:DMPG,	LE	14.9 ± 1.5	8.1 ± 0.8
50:50 DPPC-d62:DMPG-d54	LC	30.2 ± 1.6	5.0 ± 1.8
20:80 DPPC:DPPG-d62	LC	29.6 ± 2.2	5.9 ± 1.0

The mean values of π_0 and $\Delta\pi$ are calculated from three independent measurements.

The above results were obtained for binary lipid mixtures where the PG component featured a hydrocarbon chain, which is shorter than that of the PC component by two methylene groups, thus exhibiting a non-ideal mixing behavior. To explore whether the different protein binding observed for 30% DMPG is due to the non-ideal mixing of the two lipid components in the LC phase, we repeated this experiment by IRRAS, but, this time, for a mixture where both PG and PC chains had the same lengths. The isotherms of these mixtures (Fig. 1) indicated that the sample 70:30 DMPG:DMPC (both lipids with C_{14} chains) was in the LE phase at π = 30 mN/m, whereas the sample 70:30 DPPC-d62:DPPG (both lipids with C_{16} chains) was in the LC phase at this pressure. Interestingly, these two samples did not show any significant difference in protein binding at π = 30 mN/m (Fig. 5 and Table 5). This result suggests that the non-ideal mixing of the lipids accounts for the differences in protein binding.

DISCUSSION

The most striking result of this study is the phase-state dependence of protein binding to monolayers for samples

TABLE 4 Characterization of the monolayer after cytochrome c (cyt c) adsorption as obtained from three-layer model fits to the NR data

Sample	Lipid Phase	[cyt c]/nM	d_{Ch}/Å	$\rho_{Ch}/10^{-6}$ Å^{-2}	d_{Hd}/Å	$\rho_{Hd}/10^{-6}$ Å^{-2}	d_{Pr}/Å	$\rho_{Pr}/10^{-6}$ Å^{-2}	η_{Pr}/%
70:30 DPPC-d62:DMPG	LE	420 ± 30	13.0 ± 2.0	5.18 ± 0.22	8.0	3.85 ± 0.20	26.0 ± 0.7	5.53 ± 0.06	20.2 ± 1.8
	LC	420 ± 30	16.3 ± 2.2	5.05 ± 0.12	8.0	3.98 ± 0.09	26.9 ± 1.5	5.10 ± 0.04	32.2 ± 1.5
50:50 DPPC-d62:DMPG	LE	420 ± 30	13.0 ± 2.0	4.21 ± 0.18	8.0	3.70 ± 0.26	26.0 ± 1.5	5.00 ± 0.04	36.5 ± 1.7
50:50 DPPC-d62:DMPG-d54	LC	700 ± 30	16.8 ± 1.8	5.79 ± 0.08	8.0	5.98 ± 0.23	27.0 ± 2.3	4.75 ± 0.04	41.8 ± 1.4
20:80 DPPC:DPPG-d62	LC	420 ± 30	19.7 ± 2.7	5.15 ± 0.04	8.0	4.24 ± 0.22	26.7 ± 2.1	4.55 ± 0.04	47.9 ± 1.6

Here, cyt c, cytochrome c; d_{Ch}, ρ_{Ch} respective thickness and SLD of the chain region; d_{Hd}, ρ_{Hd} of the lipid head-group region; and d_{Pr}, ρ_{Pr} of the protein layer.

The values of η_{Pr} (protein coverage) and confidence limits for the fitting results were calculated as described in the data analysis section.

containing 30% anionic PG under chain mismatch conditions, although this effect was not observed for ideal mixing conditions or for higher (50%) PG content. The phase-state dependence of water-soluble protein binding is well established for lipid bilayers on a solid support and is used for bio-separation purposes (Loidl-Stahlhofen et al., 1996). It was demonstrated that the domain formation in the gel phase of bilayers due to non-ideal mixing of its neutral and charged lipid components is the dominant contribution to this effect (Käsbauer and Bayerl, 1999). The creation of such domains with diameters of <20 nm (Gliss et al., 1998) causes an increase of the local charge density of the bilayer, rendering the electrostatic binding of oppositely charged proteins stronger and the protein packing more dense (Käsbauer and Bayerl, 1999). Despite the 2–3 orders of magnitude larger size of monolayer domains compared to those in bilayers, our results obtained for the 70:30 DPPC-d62:DMPG samples strongly suggest that the dominating mechanism that controls the electrostatic coupling of proteins to the lipid surface is similar for bilayers and monolayers.

One could be tempted to argue that the increase of lipid packing density at the LE-LC transition may provide a sufficiently high increase of the surface charge density to cause a Coulomb attraction between the oppositely charged proteins and the lipid monolayer. However, the negative result of our experiment using anionic and zwitterionic lipids of identical (C_{14}) chain length (samples 70:30 DMPC:DMPG and 70:30 DPPC-d62:DPPG) does not support this

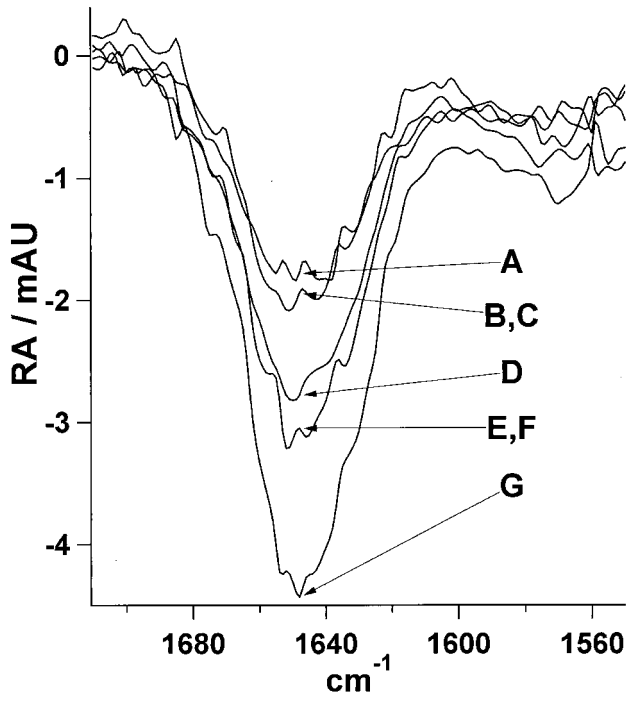

FIGURE 3 IRRAS difference spectra of the amide I region of all lipid monolayer samples studied after the adsorption of cytochrome c. A, 70:30 DPPC-d62:DMPG, LE phase; B, 70:30 DPPC-d62:DMPG; C, 70:30 DMPC:DMPG; D, 70:30 DPPC-d62:DMPG, LC phase; E, F, 50:50 DPPC-d62:DMPG, LE and LC phase; G, 20:80 DPPC:DPPG-d62.

TABLE 5 Height of the amide I absorbance peak of the infrared reflectance/absorbance spectra and protein coverage η_{Pr} for both phase states and for all monolayer samples studied

Sample	Lipid Phase	A_{mol}/Å^2	RA/mAU	η_{Pr}/%
70:30 DPPC-d62:DMPG	LE	68 ± 2	1.88 ± 0.06	20.8 ± 0.7
	LC	47 ± 1	2.70 ± 0.03	29.9 ± 0.3
70:30 DMPC:DMPG	LE	56 ± 2	1.94 ± 0.24	21.8 ± 2.8
70:30 DPPC-d62:DPPG	LC	44 ± 1	1.97 ± 0.22	21.5 ± 2.7
50:50 DPPC-d62:DMPG	LE	68 ± 2	3.16 ± 0.03	35.0 ± 0.3
	LC	49 ± 1	3.31 ± 0.05	36.6 ± 0.6
20:80 DPPC:DPPG-d62	LC	45 ± 1	4.32 ± 0.11	47.9 ± 1.2

η_{Pr} was obtained from the calibration with the NR data.

A_{mol}, area per lipid molecule obtained from three independent film balance measurements.

1 mAU (milli absorbance unit) = 10^{-3}.

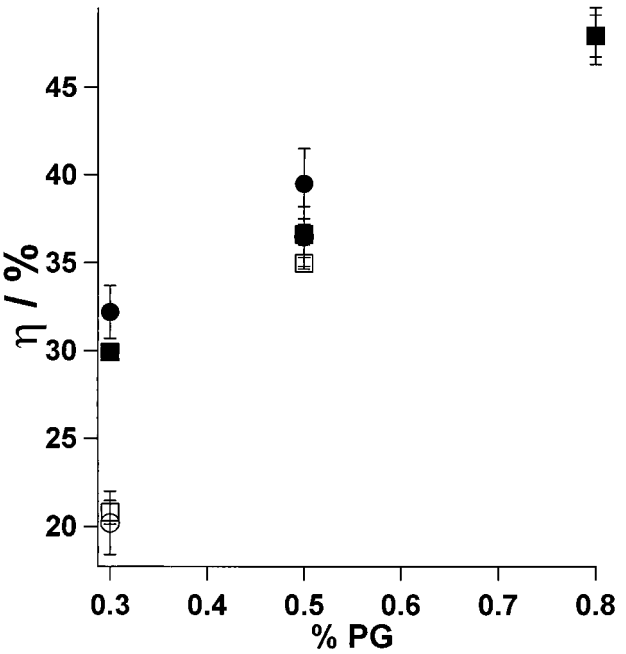

FIGURE 4 Amount of cytochrome c bound to the lipid monolayer in terms of the protein coverage η_{Pr} versus the proportion of anionic lipid in a DPPC/DMPG monolayer. η_{Pr} was determined from NR (*circles*) using Eq. 2 and from IRRAS measurements (*squares*). Open symbols represent the LE phase and full symbols the LC phase of the monolayer.

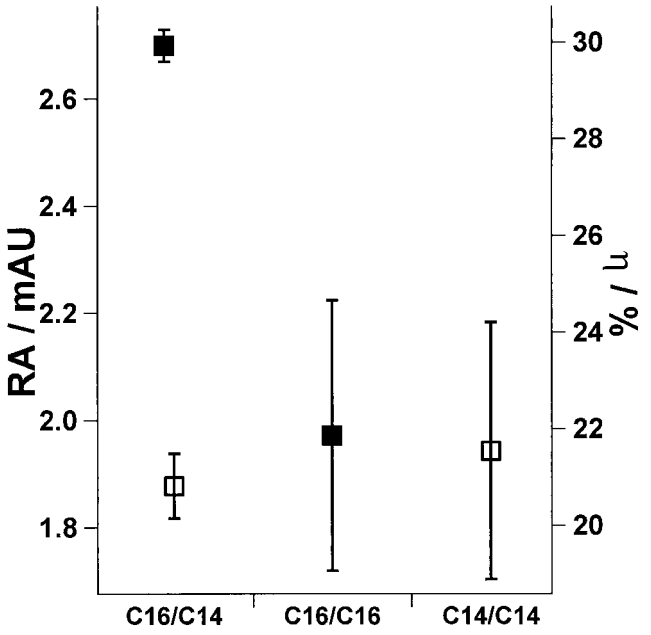

FIGURE 5 Intensity of the amide I band and protein coverage η_{Pr} as obtained from IRRAS measurements of binary lipid monolayer systems containing 30% anionic lipids for LE and LC phase and different constituent chain lengths: C16/C14: 70:30 DPPC-d62:DMPG; C16/C16: DPPC-d62:DPPG; C14/C14: DMPC/DMPG. Open symbols represent the LE phase and full symbols the LC phase of the monolayer.

surmise. On the contrary, our finding that the value of η_{PR} obtained for the chain-matched sample in the LC phase (70:30 DPPC-d62:DPPG) is identical within the experimental error to that of the 70:30 DPPC-d62:DMPG sample in the LE phase (Table 5) clearly disproves the homogeneous packing argument. Besides that, a significant contribution of closer lipid packing to the protein binding is not expected from electrostatic theory. We had previously shown that the electrostatic potential increase connected with the change of lipid packing density between the two phases (assuming homogeneous mixing) is well below the thermal energy and thus negligible (Käsbauer and Bayerl, 1999).

Therefore, domain formation in the monolayer with increasing lateral pressure seems the most likely explanation. This process can give rise to a substantial enrichment of one lipid component within the domain at the expense of the other component and thus may cause a significant increase of local charge density over the domain. Our results suggest that a chain mismatch resulting in a non-ideality of the lipid mixing is crucial for a higher protein coupling to the LC phase monolayer. Because the 3.1-nm diameter of cytochrome c is very small compared to monolayer domain sizes, we can assume that many protein molecules couple to a single domain. A prerequisite is that the charge enrichment within the domain by partial demixing is sufficiently high to provide an attractive electrostatic potential energy at or above the thermal energy. Demixing can occur when the accumulation of like lipids as next neighbors is energetically favorable over an association between unlike lipids. The underlying force is the van-der-Waals interaction between the lipid hydrocarbon chains. Two major factors tend to prevent demixing: entropy and Coulomb repulsion between like-charged lipids. In an uncharged layer, demixing would take place up to the level where the gain in energy due to like lipid interaction would make up for the loss in mixing entropy. However, in a system containing charged lipids, the Coulomb repulsion will shift this level at the expense of like neighbor interactions, depending on the percentage of the charged species in the mixture. Consequently, the closer a binary mixture comes to equimolarity the more it will reduce its tendency for demixing in a similar way as the increase of the proportion of charged lipids does. These considerations may offer a rationale for the different binding characteristics of the DPPC monolayers containing 30% and 50% DMPG: to obtain a significant demixing upon the transition to the LC phase, much more entropy would be required for compensation at 50% than at 30% DMPG. Moreover, Coulomb repulsion would provide a hindrance for demixing at 50% DMPG compared to 30% DMPG. For these reasons it is not surprising that η_{Pr} depends on the lipid monolayer phase state only for the system containing 30% DMPG and not for the one with 50%.

The results obtained with the 20:80 DPPC:DPPG-d62 sample show that, at 50% anionic lipid content, the satura-

tion level of η_{Pr} has not been reached. Because the protein coupling can be expected to be of a Langmuir-type adsorption, enhanced binding to a charge-enriched domain can well overcompensate for the weaker binding to the charge-depleted regions.

Thus, local charge enrichment is a plausible explanation for the enhanced coupling to the 70:30 DPPC:DMPG system in the LC phase in comparison to the LE phase and to 70:30 DPPC-d62:DPPG and 70:30 DMPC:DMPG samples where mixing is rather ideal. A similar saturation level of anionic lipids, above which the control of protein binding via the lipid phase state is dominated by an overall Coulomb attraction, was previously observed for the case of bilayers on a solid support (Käsbauer and Bayerl, 1999).

In spite of several similarities regarding the protein coupling to monolayers and bilayers, there are a number of distinguishing features that should be kept in mind. In bilayers, we observed a virtually complete unbinding of cytochrome c for fluid phase conditions (Käsbauer and Bayerl, 1999; Loidl-Stahlhofen et al., 1996), whereas LE phase monolayers showed merely a reduction of the bound protein fraction. Two reasons may account for these differences. One is that we used for monolayers a PG proportion which was at least a factor of 10 higher than that used in bilayers to obtain a readily detectable single layer of adsorbed protein. Second, the energy to detach the protein from the fluid monolayer surface was solely thermal in nature, whereas, for the case of bilayers, the flow of the aqueous bulk phase provided the dominating force for detachment. A further difference between monolayers and bilayers is that we determined for the former the amount of bound protein in each phase, i.e., after adjustment of the lateral pressure to the desired phase state, cytochrome c was added to the subphase and (after sufficient incubation) quantified by the measurement. In bilayers, cytochrome c was coupled to the gel phase bilayer, the amount of protein bound was quantified, then the bilayer was transferred to the fluid state by raising the temperature, and the amount of protein was quantified again. The reason for the procedure used for the monolayers is that the bound cytochrome c may stabilize the LC phase domains upon expansion to the LE state and thus prevent an effective protein detachment. Finally, the growth of domains in monolayers is rather continuous over a large pressure range above the critical point, resulting in a gradient of charge density from the domain center to the edge. In contrast, bilayer domains are exceedingly small, formed instantaneously at the transition to the gel phase, and grow in number rather than in size (Gliss et al., 1999). As a result, the composition of a single bilayer domain is most likely rather homogeneous over its diameter. Thus, the detachment of the protein upon the dispersion of the domain within the fluid bilayer will occur more rapidly than for the case of the large monolayer domain.

CONCLUSION

The results of the work strongly suggest that the domain formation in lipid monolayers consisting of binary lipid mixtures of an anionic and a neutral lipid component can alter the amount of cytochrome c that binds to the monolayer. The driving force is the demixing of the two lipid constituents at the transition from the LE to the LC phase.

Furthermore, this study shows that IRRAS measurements using a Langmuir trough shuttle system for water-vapor band compensation represent a very sensitive method for the detection of protein binding to monolayers and its changes due to variation of lipid composition and lateral pressure. The IRRAS results agree well with those obtained by NR and the combination of both techniques where NR is used for a calibration of the IRRAS data can save a substantial amount of rare and expensive neutron beam time.

The technical assistance of Martin Lieb during the neutron experiments is gratefully appreciated.

This work was supported by research grants from the Deutsche Forschungsgemeinschaft and the Bundesministerium für Bildung und Forschung.

REFERENCES

Albrecht, O., H. Gruler, and E. Sackmann. 1978. Polymorphism of phospholipid monolayers. *J. Phys. France.* 39:301–313.

Bayerl, T. M., R. K. Thomas, J. Penfold, A. R. Rennie, and E. Sackmann. 1990. Specular reflection of neutrons at phospholipid monolayers. Changes of monolayer structure and headgroup hydration at the transition from the expanded to the condensed phase state. *Biophys. J.* 57: 1095–1098.

Bertie, J. E., M. K. Ahmed, and H. H. Eysel. 1989. Infrared intensities of liquids. 5. Optical and dielectric constants, integrated intensities, and dipole moment derivatives of H_2O and D_2O at 22°C. *J. Phys. Chem.* 93:2210–2218.

Born, M., and E. Wolf. 1993. Principles of Optics. Pergamon Press, Oxford.

Brumm, T., C. Naumann, E. Sackmann, A. R. Rennie, R. K. Thomas, D. Kanellas, J. Penfold, and T. M. Bayerl. 1994. Conformational changes of the lecithin headgroup in monolayers at the air/water interface. A neutron reflection study. *Eur. Biophys. J.* 23:289–296.

Bushnell, G. W., and G. V. Louie. 1990. High-resolution three-dimensional structure of horse heart cytochrome c. *J. Mol. Biol.* 214:585–595.

Chirgadze, Y. N., O. V. Fedorov, and N. P. Trushina. 1975. Estimation of amino acid residue side chain absorption in the infrared spectra of protein solutions in heavy water. *Biopolymers.* 14:679–694.

Dluhy, R. A. 1986. Quantitative external reflection infrared spectroscopic analysis of insoluble monolayers spread at the air–water interface. *J. Phys. Chem.* 90:1373–1379.

Flach, C. R., J. W. Brauner, J. W. Taylor, R. C. Baldwin, and R. Mendelsohn. 1994. External reflection FTIR of peptide monolayer films in situ at the air/water interface: experimental design, spectra–structure correlations and effects of hydrogen–deuterium exchange. *Biophys. J.* 67: 402–404.

Gliss, C., H. Clausen-Schaumann, R. Günther, S. Odenbach, O. Randl, and T. M. Bayerl. 1998. Direct detection of domains in phospholipid bilayers by grazing incidence diffraction of neutrons and atomic force microscopy. *Biophys. J.* 74:2443–2450.

Gliss, C., O. Randl, H. Casalta, E. Sackmann, R. Zorn, and T. M. Bayerl. 1999. Anisotropic motion of cholesterol in oriented DPPC bilayers

studied by quasi-elastic neutron scattering: the liquid-ordered phase. *Biophys. J.* 77:331–340.

Johnson, S. J., T. M. Bayerl, W. Weihan, H. Noack, J. Penfold, R. K. Thomas, D. Kanellas, A. R. Rennie, and E. Sackmann. 1991. Coupling of spectrin and polylysine to phospholipid monolayers studied by specular reflection of neutrons. *Biophys. J.* 60:1017–1025.

Käsbauer, M., and T. M. Bayerl. 1999. Formation of domains of cationic or anionic lipids in binary lipid mixtures increases the coupling strength of water soluble proteins to supported bilayers. *Biochemistry.* 38: 15258–15263.

Loidl-Stahlhofen, A., S. Kaufmann, T. Braunschweig, and T. M. Bayerl. 1996. The thermodynamic control of protein binding to lipid bilayers for protein chromatography. *Nature Biotechnol.* 14:999–1002.

Macdonald, I. D. G., and W. E. Smith. 1996. Orientation of cytochrome c adsorbed on a citrate-reduced silver colloid surface. *Langmuir.* 12: 706–713.

Maierhofer, A. P., and T. M. Bayerl. 1998. The interaction of proteins with membrane surfaces at molecular resolution: the neutron reflection method. *In* Modern Optics, Electronics and High Precision Techniques in Cell Biology. G. Isenberg, editor. Springer Verlag, Berlin. 139–157.

Möhwald, H. 1995. Phospholipid monolayers. *In* Structure and Dynamics of Membranes. R. Lipowsky and E. Sackmann, editors. Elsevier Science B. V., Amsterdam. 161–211.

Nagle, J. F., and M. C. Wiener. 1988. Structure of fully hydrated bilayer dispersions. *Biochim. Biophys. Acta.* 942:1–10.

Naumann, C., T. Brumm, A. R. Rennie, J. Penfold, and T. M. Bayerl. 1995. Hydration of DPPC monolayers at the air/water interface and its modulation by the nonionic surfactant C12E4: a neutron reflection study. *Langmuir.* 11:3948–3952.

Naumann, C., C. Dietrich, A. Behrisch, T. Bayerl, M. Schleicher, D. Bucknall, and E. Sackmann. 1996. Hisactophilin-mediated binding of actin to lipid lamellae: a neutron reflectivity study of protein membrane coupling. *Biophys. J.* 71:811–823.

Naumann, C., C. Dietrich, J. R. Lu, R. K. Thomas, A. R. Rennie, J. Penfold, and T. M. Bayerl. 1994. Structure of mixed monolayers of DPPC and polyethylene glycol monododecyl ether at the air/water interface determined by neutron reflection and film balance techniques. *Langmuir.* 10:1919–1925.

Peters, R., and K. Beck. 1983. Translational diffusion in phospholipid monolayers measured by fluorescence microphotolysis. *Proc. Natl. Acad. Sci. USA.* 80:7183–7187.

Reinl, H. M., and T. M. Bayerl. 1993. Interaction of myelin basic protein with single bilayers on a solid support - An NMR, DSC and polarized infrared ATR study. *Biochim. Biophys. Acta.* 1151:127–136.